The BTB transcription factor, Abrupt, acts cooperatively with Chronologically inappropriate morphogenesis (Chinmo) to repress metamorphosis and promotes leg regeneration

Hesper Khong, Kayli Hattley and Yuichiro Suzuki

Department of Biological Sciences, Wellesley College, 106 Central St., Wellesley, MA 02481

* Corresponding author: Yuichiro Suzuki, Department of Biological Sciences, Wellesley College, 106 Central St., Wellesley, MA 02481; email ysuzuki@wellesley.edu; telephone (+01)781-283-3100

Abstract

Many insects undergo the process of metamorphosis when larval precursor cells begin to differentiate to create the adult body. The larval precursor cells retain stem cell-like properties and contribute to the regenerative ability of larval appendages. Here we demonstrate that two Broad-complex/Tramtrack/Bric-à-brac Zinc-finger (BTB) domain transcription factors, Chronologically inappropriate morphogenesis (Chinmo) and Abrupt (Ab), act cooperatively to repress metamorphosis in the flour beetle, *Tribolium castaneum*. Knockdown of *chinmo* led to precocious development of pupal legs and antennae. We show that although topical application of juvenile hormone (JH) prevents the decrease in *chinmo* expression in the final instar, *chinmo* and JH act in distinct pathways. We demonstrate that another gene encoding the BTB domain transcription factor, Ab, is also necessary for the suppression of *broad* (*br*) expression in *T. castaneum* in a *chinmo* RNAi background and that simultaneous knockdown of *ab* and *chinmo* leads to the precocious onset of metamorphosis. Furthermore, we demonstrate that knockdown of *ab* leads to the loss of regenerative potential of larval legs independently of *br*. In contrast, *chinmo* knockdown larvae exhibit pupal leg regeneration when a larval leg is ablated. Taken together, our results show that both *ab* and *chinmo* are necessary for the maintenance of the larval tissue identity and, apart from its role in repressing *br*, *ab* acts as a crucial regulator of larval leg regeneration. Our findings indicate that BTB domain proteins interact in a complex manner to regulate larval and pupal tissue homeostasis.

Keywords

Metamorphosis, limb regeneration, Chinmo, Abrupt, juvenile hormone, *Tribolium castaneum*

Graphical abstract

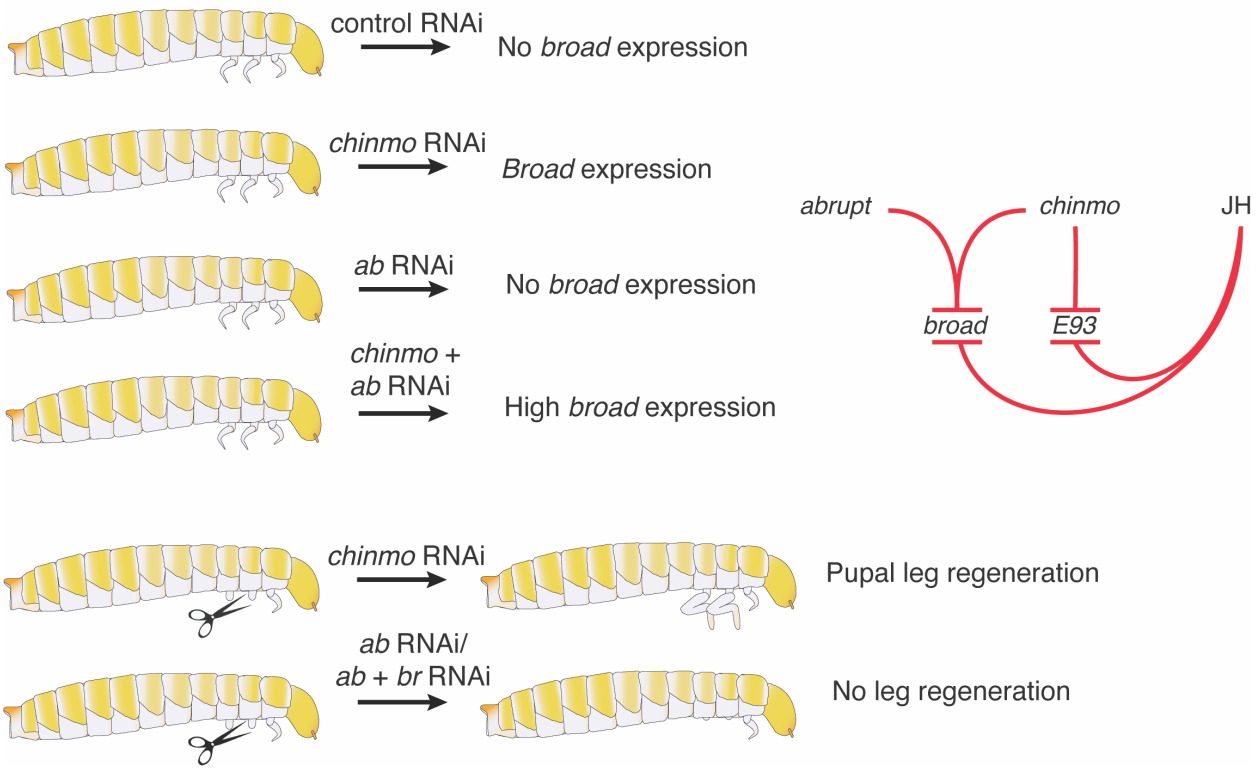

47

48

Introduction

Metamorphosis is associated with major morphological changes that lead to maturation and proliferation of adult tissues. Holometabolous insects, insects that undergo complete metamorphosis, are characterized by the presence of the larval, pupal, and adult stages. Larvae of many holometabolous insects are distinguished by the presence of precursor cells, either detected in the form of imaginal discs, tissues that are set aside during embryogenesis, or imaginal cells, cells embedded within the larval epidermal cells that proliferate during metamorphosis (Truman, 2019). These precursor cells undergo extensive proliferation and movement during metamorphosis to give rise to adult tissues. In most holometabolous insects, larval tissues also contribute to the adult body, thus contributing to the formation of both larval and adult structures. These cells can therefore be thought of as partially but not completely differentiated cells (Suzuki et al., 2019). Although holometabolous larvae are characterized by tissues with extensive regenerative abilities, many insects lose their ability to regenerate structures during metamorphosis (Suzuki et al., 2019). How the larval tissues are maintained in an undifferentiated state has important implications for our understanding of stem cell maintenance and differentiation and the evolution of holometaboly.

The hormonal control of insect metamorphosis has been explored for over a century. Two key groups of insect hormones have been identified: the sesquiterpenoid juvenile hormone (JH) and the steroid hormones, ecdysteroids (Nijhout, 1998). JH acts as a *status quo* hormone, maintaining the identity of the previous instar when ecdysteroids trigger a molt (Riddiford, 1996). Thus, topical application of JH on larvae can lead to extra larval molts (Hatakoshi et al., 1988; Parthasarathy and Palli, 2009), and injection or topical application of JH in early pupae

induces the development of a second pupal cuticle (Gilbert and Schneiderman, 1960; Riddiford and Ajami, 1973).

The molecular processes that act downstream of hormones are actively studied. JH binds to the basic helix-loop-helix (bHLH) transcription factor, Methoprene tolerant (Met) (Charles et al., 2011; Jindra et al., 2015). *Met* knockdown in the flour beetle, *Tribolium castaneum*, leads to precocious metamorphosis (Konopova and Jindra, 2007; Parthasarathy et al., 2008b). In severely affected individuals, the larvae skip the pupal stage and develop directly into adultoid animals with adult cuticles and differentiated structures albeit with dramatically reduced appendage sizes (Parthasarathy et al., 2008b). Once bound by JH, Met, in turn, activates the JH response gene, *Krüppel homolog 1* (*Kr-h1*). Similar to *Met* knockdown larvae, precocious adult development commences when *Kr-h1* expression is knocked down (Minakuchi et al., 2009). *Kr-h1* is upregulated by JH and is present at high levels throughout much of the larval stage but drops in the final larval stage when JH levels also drop (Minakuchi et al., 2009). Once the JH level drops in the final larval instar, the pupal specifier gene encoding the Broad-complex/Tramtrack/Bric-à-brac Zinc-finger/poxvirus and zinc finger (BTB/POZ) family transcription factor, Broad (Br), is upregulated (Zhou et al., 1998; Zhou and Riddiford, 2001). Br is necessary and sufficient for the appearance of pupal structures in holometabolous insects (Konopova and Jindra, 2008; Parthasarathy et al., 2008a; Suzuki et al., 2008; Zhou and Riddiford, 2002). Topical application of JH leads to extra larval molts and inhibition of *br* expression (Suzuki et al., 2008). When *br* is knocked down in *T. castaneum* larvae, the prepupa molts into a larval-adult intermediate that lacks pupal traits (Konopova and Jindra, 2008; Suzuki et al., 2008). Finally, the adult specifier gene *ecdysone-induced protein 93F* (*E93*) promotes the differentiation of adult structures: Knockdown of *E93* prevents adult differentiation and leads to the retention of pupal

94 characteristics (Urena et al., 2014). *E93* represses the expression of *Kr-h1* and *br* in the pupal
95 stage, leading to the development of the adult stage (Urena et al., 2014).
96 Recent studies in *D. melanogaster* have demonstrated that another BTB domain
97 transcription factor, Chronologically inappropriate morphogenesis (Chinmo), acts as a larval-
98 specific stage specifier (Chafino et al., 2023; Truman and Riddiford, 2022). Chinmo was
99 identified as a gene that maintains the temporal identity of neurons in the brain: Loss of Chinmo
100 leads to early-born neurons adopting the fate of a late-born neuron at an early developmental
101 stage (Zhu et al., 2006). Its removal leads to the precocious expression of Br in the nervous
102 system and the imaginal discs, precocious imaginal disc growth, and appearance of pupal traits in
103 first instar *D. melanogaster* larvae (Narbonne-Reveau and Maurange, 2019; Truman and
104 Riddiford, 2022). Independent of its role in repressing precocious *br* expression, Chinmo also
105 acts on the tissues to promote their growth and maturation (Chafino et al., 2023). Although there
106 are conflicting observations, when *chinmo* is removed, *E93* has also been reported to be
107 upregulated in the imaginal discs of first instar larvae (Truman and Riddiford, 2022; but see also
108 Chafino et al., 2023). When overexpressed, *chinmo* can repress *E93* during the pupal period and
109 prevent adult differentiation (Chafino et al., 2023). This role of *chinmo* in repressing *E93*
110 expression is also conserved in the cockroach, *Blattella germanica*, a hemimetabolous insect:
111 When *chinmo* is knocked down in L4 nymphs, the nymphs molt once before precociously
112 molting into an adult (Chafino et al., 2023).
113 In addition to regulating the timing of metamorphic transitions, *chinmo* has been
114 implicated in imaginal disc regeneration. Imaginal discs in *D. melanogaster* have an extensive
115 ability to regenerate (Bryant, 1971; Fox et al., 2020; Schubiger, 1971). Recent studies in *D.*
116 *melanogaster* have demonstrated that during metamorphosis, imaginal discs lose their ability to

117 regenerate (Karanja et al., 2022; Narbonne-Reveau and Maurange, 2019). This event is mediated
118 by the steroid hormones, ecdysteroids (Karanja et al., 2022). During the middle of the final
119 instar, ecdysone inhibits the expression of *chinmo* and activates the expression of *br* (Narbonne-
120 Reveau and Maurange, 2019). Chinmo promotes regeneration of imaginal discs whereas
121 activation of Br leads to the loss of regenerative potential and onset of differentiation (Narbonne-
122 Reveau and Maurange, 2019).

123 Chinmo has been shown to have many functional similarities with Abrupt (Ab), another
124 BTB domain transcription factor. Both Chinmo and Ab have been indicated to act as oncogenes
125 and their overexpression blocks differentiation and leads to the maintenance of progenitor-like
126 state in various tissues (Doggett et al., 2015; Turkel et al., 2013). Importantly, like Chinmo, Ab
127 is temporally regulated in muscles, neuromuscular junctions, and α′/β′ to α/β neuronal transitions
128 in the mushroom body, and its expression must be repressed for the tissues to terminally
129 differentiate (Caygill and Johnston, 2008; Kucherenko et al., 2012). Both Ab and Chinmo are
130 regulated by the heterochronic microRNA, *let-7* (Caygill and Johnston, 2008; Wu et al., 2012).
131 Finally, Chinmo and Ab have been shown to play functionally overlapping roles, and the roles of
132 Chinmo can be unmasked when the function of Ab is compromised (Doggett et al., 2015). These
133 studies suggest that Ab and Chinmo act cooperatively to maintain the larval stage in *D.*
134 *melanogaster*.

135 Although *D. melanogaster* is an excellent genetic model system, it has a rather unusual
136 physiology where JH plays minimal developmental roles (Riddiford and Ashburner, 1991). In
137 many other insect species, JH plays a prominent role in regulating the timing of metamorphosis
138 and pupal commitment. In this study, we sought to examine the role of Chinmo and Ab in the
139 regulation of metamorphosis of *T. castaneum*. *T. castaneum* is a holometabolous insect with

140 physiological regulation of metamorphosis that is more typical of other insects. Although the
141 function of Ab has been studied during metamorphosis and leg regeneration of *T. castaneum*
142 (Angelini et al., 2012, 2009; Lee et al., 2013; Ravisankar et al., 2016), the role of Chinmo has not
143 yet been reported. In *T. castaneum*, *ab* knockdown larvae metamorphose at the normal
144 developmental time but develop into adults with appendage patterning defects: In the *ab*
145 knockdown adults, wings are severely reduced in size, the antennal segments are fused, and the
146 tarsal segments of the legs are lost or fused (Angelini et al., 2012, 2009; Ravisankar et al., 2016).
147 The larval appendages of *T. castaneum* allow us to probe the mechanism of stem cell-like cell
148 proliferation and differentiation (Chou et al., 2019; Suzuki et al., 2019). The first step of limb
149 regeneration is the formation of a blastema, a bump that comprises an epidermal layer with
150 precursor cells that give rise to the regenerating limb (Suzuki et al., 2019). When larval legs are
151 ablated, *ab* knockdown larvae fail to form a blastema and cannot regenerate their legs (Lee et al.,
152 2013). Since larval legs develop in *ab* knockdown embryos, the inability to regrow their legs
153 suggests that *ab* plays a regeneration-specific role, possibly by promoting the proliferation of
154 progenitor-like cells in the developing blastema (Lee et al., 2013).

155 Here we examined the roles of Ab and Chinmo in the regulation of metamorphosis and
156 larval leg regeneration in *T. castaneum* larvae. Using RNA interference (RNAi), we demonstrate
157 that *chinmo* represses *br* and *E93* expression in *T. castaneum* larvae, preventing premature pupal
158 differentiation of appendages. Moreover, through the simultaneous knockdown of *chinmo* and
159 *ab*, we reveal that *ab* also represses *br* and show that simultaneous knockdown of *ab* and *chinmo*
160 can lead to precocious metamorphosis. The expression of *chinmo* is not dependent on JH,
161 however. Independently of its role in regulating *br* expression, we show that *ab* is also necessary

for regenerative growth of larval legs. These findings support the growing evidence for BTB domain proteins in regulating distinct tissue states.

Methods

Animal husbandry

The GA1 and Pu11 strains of *T. castaneum* were used in this study. The strains were maintained in 95% whole wheat flour and 5% wheat germ. Unless otherwise noted, larvae were maintained at 29.5°C and 60% relative humidity.

cDNA synthesis and PCR amplification

RNA was isolated from whole bodies following standard Trizol extraction. The RNA was purified using RQ1 RNase-Free DNase (Promega) according to the manufacturer's instructions. cDNA was synthesized from 1 µg of RNA using the First Strand cDNA Synthesis Kit (Thermo Fisher Scientific). Primers were designed to amplify the *ab* (GenBank accession number XM_969854.4), *chinmo* (GenBank accession number XM_015980027.1) and *br* core (NM_001111264.1) through PCR (Table 1). To minimize off-target effects, the sequences targeted by these primers were blasted in iBeetle Blast (https://ibeetle-base.uni-goettingen.de/blast/). No stretches of nucleotide sequences greater than 17 bp were found outside the targeted region. The *ab* and *chinmo* sequences were also aligned using Emboss Water (Madeira et al., 2022). The output of the alignment is shown in Supplemental Fig. S1. A protein tree of Chinmo and Ab is shown in Supplemental Fig. S2.

dsRNA synthesis

For dsRNA synthesis, the amplified PCR product was purified and subsequently cloned into pCR-4 TOPO-TA vector. *E. coli* cells were transformed with this vector and grown overnight. Following extraction using the QIAprep Spin Miniprep Kit (Qiagen), the plasmids were

sequenced and linearized using Spe1 and Not1 restriction enzymes (NE Biolabs). Single-stranded RNA (ssRNA) was generated using the T3 and T7 MEGAscript Kits and the purified linearized plasmids as the templates. The ssRNA was purified and annealed according to Hughes and Kaufman (2000). The annealed product was analyzed by agarose gel electrophoresis.

Phenotypic characterization of dsRNA-injected larvae

Sixth instar larvae were injected with 0.5µL of 2 µg/µL *chinmo* dsRNA, 0.5µL of 4 µg/µL *chinmo* dsRNA, 0.5µL of 2 µg/µL *ab* dsRNA, 0.5µL of a combined solution of 2 µg/µL *ab* dsRNA and 2 µg/µL *chinmo* dsRNA, 0.5µL of a combined solution of 2 µg/µL *chinmo* dsRNA and 2 µg/µL *br* dsRNA, and 0.75µL of a combined solution of 2 µg/µL *chinmo* dsRNA, 2 µg/µL *ab* dsRNA, and 2 µg/µL *br* dsRNA. Larvae were also injected with 0.5µL of 2 µg/µL amp^r dsRNA as an injection control. Initial results obtained when *chinmo* dsRNA-injected larvae were kept at 29.5°C led to variable phenotypic effects with increasing severity with longer time to molt. To obtain robust phenotypic effects more consistently, larvae were transferred to 26°C post-dsRNA injection. To observe the effects of *ab*, *chinmo* and *br* on larval leg regeneration, larvae were injected with 0.5µL of 4 µg/µL *chinmo* dsRNA, 0.5µL of 2 µg/µL *ab* dsRNA, 0.5µL of a combined solution of 2 µg/µL *ab* dsRNA and 2 µg/µL *br* dsRNA, 0.5µL of a combined solution of 2 µg/µL *chinmo* dsRNA and 2 µg/µL *br* dsRNA, or 0.5µL of 2 µg/µL amp^r dsRNA.

Analysis of feeding behavior

Sixth instar larvae were injected with 0.5 µL of 4 µg/µL *chinmo* dsRNA or 0.5µL of a combined solution of 2 µg/µL *ab* dsRNA and 2 µg/µL *chinmo* dsRNA. Control larvae were injected with 4 µg/µL amp^r dsRNA. Larvae were maintained at 26°C on regular 95% whole wheat/5%

nutritional yeast mixture. Upon molting to the next instar, larvae were placed on the same flour mix containing 0.1 g of carmine/g of flour. The guts were dissected two days later and imaged in phosphate-buffered saline (0.02 M phosphate, 0.15 M NaCl, 0.0038 M NaH_2PO_4, 0.012 M Na_2HPO_4; pH 7.4).

Methoprene treatment

To determine the effect of methoprene on the expression of *ab* and *chinmo*, 0.5 µL of the JH analog methoprene (60 or 120 µg/µL in acetone) was ectopically applied to the dorsal side of day 0 final instar larvae. Control larvae were treated with 0.5 µL of acetone. To determine whether *ab* and *chinmo* act downstream of JH, sixth instar larvae were injected with either 0.5 µL of 4 µg/µL *chinmo* dsRNA or 0.5 µL of a combined solution of 2 µg/µL *ab* dsRNA and 2 µg/µL *chinmo* dsRNA and treated with 0.5 µL of methoprene (30 or 60 µg/µL in acetone) or 0.5 µL of acetone on the dorsal side.

Quantitative PCR (qPCR)

Sixth instar larvae were injected with 0.5µL of 2 µg/µL *chinmo* dsRNA, 0.5µL of 4 µg/µL *chinmo* dsRNA, 0.5µL of 2 µg/µL *ab* dsRNA, 0.5µL of a combined solution of 2 µg/µL *ab* dsRNA and 2 µg/µL *chinmo* dsRNA, 0.5µL of a combined solution of 2 µg/µL *chinmo* dsRNA and 2 µg/µL *br* dsRNA, 0.75µL of a combined solution of 2 µg/µL *chinmo* dsRNA, 2 µg/µL ab dsRNA, and 2 µg/µL *br* dsRNA, and 0.5µL of 2 µg/µL amp^r dsRNA. Larvae were kept at 29.5°C and collected three days later. To examine how the *chinmo* expression might be altered in response to *Met*, *Kr-h1* and *jhamt3* RNAi, day 2 fifth instar larvae were injected with dsRNA and collected on day 3 of the sixth instar so that the genes were sufficiently knockdown. All collected

larvae were immediately placed in Trizol and frozen. RNA was converted to cDNA as described above. For qPCRs, SsoAdvanced SYBR Green Supermix (Bio-Rad) was used with primers listed in Table 1. Three to four biological replicates, each containing two injected larvae, were used, and each biological replicate was run in triplicates. The standard curve method was used to analyze the data.

Knockdown verification

To confirm the knockdown of *ab* and *chinmo* expression, day 0 sixth instar larvae were injected with *ab*, *chinmo* and amp^r dsRNA and kept at 29.5°C for three days. Larvae were then placed in Trizol and RNA was isolated as described above. To verify knockdown, semi-quantitative PCR was used. For *RP49*, 20, 25, and 30 cycles were used. For *chinmo*, 30, 35 and 40 cycles were used (Supplemental Fig. S2).

Results

Chinmo *suppresses precocious metamorphosis of legs and antennae*

To investigate the role of *chinmo* in *T. castaneum*, *chinmo* dsRNA was injected into sixth instar larvae. *chinmo* dsRNA-injected larvae exhibited larval-pupal mosaic phenotypes characterized by lengthened or broadened legs with patches of reddish-brown discoloration (Fig. 1-2; Table 2). *Chinmo* knockdown also impacted the morphology of the antennae, which became broader and longer (Fig. 3; Table 2). The morphological alterations, especially in the legs, appeared to be partial pupal transformations (see additional evidence below). Aside from the leg and antennal morphology, however, the *chinmo* knockdown larvae did not exhibit any major alterations. The molted larvae failed to show signs of growth, possibly indicating internal alterations. Using flour containing red food coloring, we found that *chinmo* knockdown larvae did not feed (N=5; Fig. 3F). Since prepupae and pupae do not feed, the lack of feeding may reflect behavioral changes associated with precocious metamorphosis.

chinmo *and* ab *act cooperatively to suppress precocious metamorphosis*

Because *chinmo* knockdown alone was insufficient to completely transform larval structures to pupal structures, sixth instar larvae were injected with either *ab* dsRNA or a combination of *chinmo* and *ab* dsRNA. *ab* knockdown alone did not yield any obvious morphological defects although occasional larvae failed to completely shed their cuticle. When *chinmo* and *ab* dsRNA were co-injected, larvae had deformed limbs with discoloration. On the dorsal side, we observed projections at the base of the lateral bristles reminiscent of those found on pupae (Fig. 1O’’’, blue dotted circles; Fig. 5B’, 5B’’). These larvae also did not eat (N=4; Fig. 3F). In a subset of larvae (4 out of 22), we observed wing-like projections in the second and third thoracic segments although these were very small and never exhibited any wing-specific

morphologies (Fig. 1O'). To investigate these projections further, we knocked down *chinmo* and *ab* in the sixth instar Pu11 larvae, which express GFP in the wing imaginal cells under the control of a *nubbin* enhancer (Clark-Hachtel et al., 2013). Intriguingly, GFP was not detected in these tissues, indicating that despite the presence of projections, *nubbin* is not expressed (n=4; Fig. 3G, H). To rule out the possibility that *ab* knockdown alone, which leads to miniature wings (Ravishankar et al., 2016), might lead to the absence of GFP expression, we examined the GFP expression in *ab* knockdown Pu11 prepupa and pupa. GFP was strongly expressed in these *ab* knockdown animals (Fig. 3I-I'') indicating that the absence of GFP in *chinmo* + *ab* knockdown cannot be attributed to the reduction of *ab* expression alone. Compound eyes were also absent in the *chinmo* or *chinmo* + *ab* knockdown larvae (Fig. 2). Interestingly, a fraction (8 out of 22) of *ab* + *chinmo* knockdown larvae underwent precocious metamorphosis and developed into a prepupa without a molt (Fig. 4; Table 2). This occurred without notable delay (Fig. 4), indicating that the entry into prepupal stage was unlikely to be mediated by starvation-induced precocious metamorphosis (Chafino et al., 2019). Four out of eight of these prepupae underwent pupation generating pupae with severely reduced wings and poorly developed gin traps (Fig. 5A). To determine whether *ab* + *chinmo* removal can also produce pupal traits, fifth instar larvae were co-injected with *ab* and *chinmo* dsRNA. These larvae also exhibited pupal traits (Table 2; Fig. 5E-E'') and one was also capable of progressing to the prepupa although this individual subsequently molted into an animal with both larval and pupal traits (Table 2; Fig. 5C-D'').

Chinmo *and* ab *act cooperatively to repress* br *expression*

Recent studies in *D. melanogaster* have demonstrated that Chinmo represses Br to maintain the larval stage (Chafino et al., 2023; Truman and Riddiford, 2022). Other studies have also implicated *ab* as a repressor of *br* expression. To examine how *br* expression might be

296 regulated in *T. castaneum*, we injected 1 µg of *chinmo* and 1 µg of *ab* dsRNA at the onset of the
297 sixth instar and examined the expression of *br* core region, which is shared across all *br* isoforms
298 (Konopova and Jindra, 2008; Suzuki et al., 2008). Knockdown of *chinmo* led to elevated
299 expression of *br* core, although knockdown of *ab* alone did not lead to upregulation of *br* core
300 (Fig. 6A). When 1 µg of *ab* dsRNA and 1 µg of *chinmo* dsRNA were simultaneously injected, *br*
301 core expression was significantly elevated relative to those injected with 1 µg of *chinmo* dsRNA
302 alone. While not statistically significant, this expression was slightly higher than that of larvae
303 that were injected with 2 µg of *chinmo* dsRNA. Similar trends were observed for the *br-Z3*
304 isoform (Fig. 6B). These results indicated that although *chinmo* is necessary for *br* suppression,
305 *ab* acts cooperatively with *chinmo* to further suppress *br* expression.

306 To determine whether co-injection of *br* dsRNA would prevent the appearance of pupal
307 traits, we conducted *chinmo* + *br* double knockdowns and *chinmo* + *ab* + *br* triple knockdowns.
308 In both treatments, the larvae were affected less severely than those injected with either *chinmo*
309 dsRNA or *chinmo* + *ab* dsRNA. In addition, the larval leg occasionally transformed into a leg
310 with a morphology that is characteristic of larval-adult intermediate phenotypes that develop
311 when *br* dsRNA-injected prepupae molt (Fig. 2F; Konopova and Jindra, 2008; Parthasarathy et
312 al., 2008a; Suzuki et al., 2008). Thus, the observed precocious appearance of pupal traits is likely
313 due to the activity of *br*. Taken together, our results show that both *ab* and *chinmo* act
314 cooperatively to suppress the expression of *br* and that their simultaneous removal can lead to
315 pupal transformation.

316 We also examined the expression of the JH response gene, *Kr-h1,* and the adult specifier
317 gene, *E93*. *Kr-h1* expression was not altered in the *chinmo, ab*, or *chinmo* + *ab* knockdown
318 larvae (Fig. 6D; One way ANOVA: $p=0.796$). *E93* was significantly elevated in larvae injected

with 2 µg *chinmo* dsRNA, while a modest increase was also observed in larvae injected with 1 µg *chinmo* dsRNA and those injected with 1 µg *chinmo* + 1 µg *ab* dsRNA (Fig. 6C). No increase was detected in those injected with *ab* dsRNA alone (Fig. 6C).

Finally, we explored the possibility that *chinmo* and *ab* might cross-regulate each other. We therefore examined the expression of *ab* and *chinmo* in *chinmo* and *ab* knockdown larvae, respectively. No change was observed in *chinmo* expression when *ab* was knocked down (Fig. 6E). *ab* was slightly decreased when *chinmo* was knocked down although this difference was not statistically significant (Fig. 6F). Therefore, *ab* is unlikely to regulate the expression of *chinmo* and the enhanced expression of *br* and *E93* is not due to an indirect effect of *ab* RNAi on *chinmo* expression.

JH and chinmo *interaction*

In *T. castaneum*, JH maintains the larval stage, and topical application of JH leads to supernumerary larval molts. Chinmo could act upstream or downstream of JH. To determine whether JH might act upstream of *chinmo*, larvae were injected with *chinmo* dsRNA and the JH analog methoprene was ectopically applied. We found that even in the presence of methoprene, the larvae exhibited the *chinmo* knockdown phenotype with malformed legs and antennae similar to acetone-treated *chinmo* knockdown larvae (Table 3; Fig. 7A, B). Similarly, JH did not ameliorate the phenotypes obtained through the double knockdown of *ab* and *chinmo* (Table 3; Fig. 7C). A subset of *chinmo* + *ab* double knockdown larvae (2 out of 6 treated with 15 µg methoprene; 1 out of 5 treated with 30 µg methoprene) entered the prepupal stage even when they were treated with methoprene. When methoprene was topically applied to day 0 final instar *T. castaneum* larvae, both *chinmo* and the JH response gene *Kr-h1* expression was significantly

342 higher than those treated with acetone. In contrast, *ab* expression was not significantly altered by
343 methoprene (One-way ANOVA: p=0.543).

344 We next examined whether *chinmo* expression might be altered when JH signaling is
345 disrupted. Because larvae injected with *Met*, *Kr-h1* or *jhamt3* dsRNA often undergo one or two
346 additional molts before undergoing precocious metamorphosis (Konopova and Jindra, 2007;
347 Minakuchi et al., 2008; Minakuchi et al., 2009), larvae were injected with dsRNA on day 2 of the
348 fifth instar and allowed to molt to the sixth instar before the expression was analyzed on day 3.
349 Neither the expression of *chinmo* nor *ab* was altered by the knockdown of *Met*, *Kr-h1* or *jhamt3*
350 (Fig. 7G, H). Taken together, these experiments demonstrate that JH is sufficient to maintain
351 high *chinmo* expression in the final instar but is not necessary for *chinmo* or *ab* expression.

352

353 *Ab, but not Chinmo, is necessary for larval regeneration in* T. castaneum *legs*

354 To investigate the regenerative role of *chinmo*, *chinmo* was knocked down in the sixth
355 instar and legs were ablated on the following day. In *amp*^{r} dsRNA-injected control larvae, when
356 legs were ablated one day after injection and left at 26°C, the larvae molted and regenerated their
357 legs (Table 4; Fig. 8A). When *chinmo* was knocked down, the larvae also regenerated their legs
358 (Table 4). In *chinmo* knockdown larvae that took longer to molt and therefore had a greater
359 amount of time to regenerate, the regenerated legs assumed a pupa-like leg morphology (Fig.
360 8B). These legs more closely resembled pupal legs compared to the unablated legs, suggesting
361 that the reduction of *chinmo* and hence upregulation of *br* did not alter their ability to regenerate.
362 Thus, although Chinmo has been shown to be necessary for regenerative proliferation, and *br* has

363 previously been shown to inhibit regeneration in *D. melanogaster* wings, in *T. castaneum*, legs
364 can regenerate even when *chinmo* expression is reduced and *br* expression is elevated.

365 In contrast, as previously reported, *ab* knockdown larvae failed to regenerate the larval
366 legs after a molt (Lee et al., 2013) (Table 4; Fig. 8C). To determine whether this is due to the
367 expression of *br*, *ab* and *br* were simultaneously knocked down and the legs were removed one
368 day later. These *ab* + *br* double knockdown larvae still failed to regenerate their legs (Table 4;
369 Fig. 8D), indicating that the inability of *ab* knockdown larvae to regenerate their legs is not due
370 to precocious upregulation of *br*. These findings indicate that in *T. castaneum*, the primary
371 regulator of blastema formation and proliferation is Abrupt, not Chinmo.

372 To determine whether JH signaling is involved in this *ab*-dependent regenerative
373 potential, we examined whether JH signaling was necessary for the regeneration of larval legs.
374 Day 2 fifth instar larvae were injected with *jhamt3*, *Kr-h1* or *Met* dsRNA and their legs were
375 subsequently ablated on day 1 of the sixth instar. Although the larvae initiated metamorphosis
376 without molting, all of the animals that eventually developed into adults had regenerated their
377 legs (n=4 for each treatment; Fig. 9). These results indicate that JH signaling is not necessary to
378 promote larval leg regeneration and that the role of Ab in promoting larval leg regeneration is
379 independent of JH signaling.

380

381

Discussion

In this study, we investigated the roles of two genes encoding the BTB domain transcription factors, *chinmo* and *ab,* in the regulation of metamorphic timing and larval leg regeneration. We found that *chinmo* knockdown alone causes the larval appendages to begin to adopt pupal identities. Knockdown of both *ab* and *chinmo* caused more extensive pupal transformation and de-repressed *br* expression.

Chinmo and ab act cooperatively to regulate the timing of metamorphosis

Knockdown of *chinmo* alone caused alterations to the antennae and legs after the first molt. Especially given that the regenerated leg in *chinmo* knockdown larvae exhibit pupal morphology (Fig. 8B) and *chinmo* knockdown larvae had elevated *br* expression (Fig. 6A,B), the alterations we observed are likely partial pupal transformations. The *chinmo* knockdown larvae also stopped feeding after the molt (Fig. 3F), indicating that the effects of knockdown extend beyond the appendages. When *chinmo* is knocked down in *D. melanogaster*, a pupal cuticle is induced in the epidermis (Truman and Riddiford, 2022). The imaginal discs also express *br* and begin to proliferate in late first instar larvae, suggesting precocious metamorphic entry of these tissues (Chafino et al., 2023; Truman and Riddiford, 2022). Thus, in *D. melanogaster*, both tissues begin precocious metamorphosis albeit at slightly different developmental time points. In *T. castaneum*, *chinmo* knockdown had the strongest visible effects on the appendages although given the similarity between the larval and pupal cuticle, it is difficult to know whether slight pupal characteristics were also induced in the epidermis of the *chinmo* knockdown larvae.

We found that the knockdown of *ab* augments the effects of *chinmo* knockdown by inducing higher expression of *br* and causing whole-body transformations. Since the effects of

injecting 1 µg *chinmo* and 1 µg *ab* dsRNA are more severe than those seen after the injection of 2 µg *chinmo* dsRNA, we suspect that *ab* and *chinmo* likely act synergistically to regulate the expression of *br*. In *D. melanogaster*, both *ab* and *chinmo* have been shown to modulate the temporal transition of the nervous system during metamorphosis (Kucherenko et al., 2012; Wu et al., 2012; Zhu et al., 2006). Thus, we suspect that the roles of *chinmo* and *ab* in regulating the timing of pupal commitment are conserved between the two species. Curiously, although the legs and antennae were affected, the alternations to structures that develop *de novo* during metamorphosis were either not affected or only minimally impacted. For example, compound eyes did not develop, and only miniature wing-like projections developed. The use of Pu11 larvae demonstrated that the wing-like projections do not express *nubbin*, a key wing gene. Wing cells in *T. castaneum* are contributed by both the cells in the notum and the pleural plates (Clark-Hachtel et al., 2013). The pleural cells do not express *nubbin* whereas the notum expresses *nubbin*. Thus, the absence of GFP expression in the *chinmo* + *ab* knockdown Pu11 strain suggests that the notum cells are not present in the wing-like projections. These observations suggest that knockdowns of *chinmo* or *chinmo* + *ab* are not sufficient to trigger the development of tissues that begin to proliferate *de novo* during metamorphosis. In contrast, larval structures that transform into adult structures can undergo metamorphosis when *chinmo* and *ab* are knocked down. In holometabolous insects, three different types of cells have been identified: the larva-specific cells, which only contribute to larval structures and are subsequently eliminated during metamorphosis; the polymorphic cells, which contribute to both larval and adult structures; and the imaginal cells, which proliferate during metamorphosis and contribute to the adult structures (Tanaka and Truman, 2005). We propose that during the larval stage, the knockdown of *chinmo* inhibits the proliferation of imaginal cells, similar to what has been seen

in *D. melanogaster* imaginal discs (Fig. 10A; Chafino et al., 2023). In *D. melanogaster*, in the absence of *chinmo*, *br* is upregulated and prevents the growth of imaginal discs in the larvae (Chafino et al., 2023). In many holometabolous insects, JH acts as an inhibitor of imaginal cell proliferation (Truman et al., 2006; Villarreal et al., 2015). Thus, JH and Chinmo may act in concert to regulate the proper timing of imaginal cell proliferation (Fig. 10A). In contrast, polymorphic cells and the pre-existing nervous system are prevented from transforming into pupal or adult cells due to the expression of *chinmo* and *ab* (Fig. 10B). When *chinmo* is knocked down, *br* is induced, leading to the partial pupal transformation we observed.

In addition to inducing pupal appendages, *chinmo* knockdown led to the appearance of reddish-brown pigmentation in parts of the legs and antennae. Given that the knockdown of *chinmo* also led to the upregulation of *E93*, we suspect that melanin production may be upregulated, leading to partial activation of adult-specific genes. Adult beetles are reddish black due to the production of melanin and N-β-alanyldopamine in the cuticle (Arakane et al., 2009; Kramer et al., 1984). Similar phenotypes were also obtained when *Kr-h1* was knocked down in *T. castaneum* larvae (Minakuchi et al., 2009). *Chinmo* knockdown in the larvae therefore appears to cause a precocious activation of both pupal and adult-specific genes. In the cockroach *B. germanica*, *chinmo* also represses *E93*, and its removal leads to precocious onset of adult development (Chafino et al., 2023). Our findings corroborate the notion that *chinmo* is required for juvenile tissue identity and its removal leads to precocious activation of pupal and adult tissues.

JH is not necessary for chinmo *expression*

We established that Chinmo does not act upstream of JH as *chinmo* or *ab* + *chinmo* knockdown larvae treated with methoprene yielded phenotypes similar to those treated with acetone (Fig. 7). Topical application of methoprene in the final instar maintained significantly higher expression of *chinmo* relative to those treated with acetone (Fig. 7). Moreover, knockdown of *chinmo* or *ab* + *chinmo* did not cause *Kr-h1* expression to differ across the different knockdown treatments (Fig. 6D). These results show that *chinmo* is not an upstream regulator of JH signaling. However, knockdowns of JH biosynthesis or signaling genes did not alter the expression of *chinmo* (Fig. 7), demonstrating that JH is not necessary for *chinmo* expression. This indicates that the elevated *chinmo* expression in response to topical application of JH in the final instar may be a secondary effect due to the maintenance of the larval identity, not a direct effect of JH on *chinmo* transcription.

In developing ovaries, ecdysone triggers the migration of cells known as border cells. These cells originate in the follicle cells and migrate to the oocytes. The regulation of the timing of this migration has been studied in *D. melanogaster*. In the ovaries of *D. melanogaster*, Ab appears to repress the activity of Taiman (Tai), preventing the ecdysone-mediated border cell migration. Ab binds directly to the bHLH domain of Tai, which is an activator of ecdysone signaling. Ecdysone represses Abrupt expression, allowing Tai to promote border cell migration (Jang et al., 2009). Although we do not know if Ab binds to Tai during the larval stage metamorphosis, it is interesting to note that *T. castaneum* Tai has been shown to bind to *T. castaneum* Met, the JH receptor (Jindra et al., 2021). Knockdown of one of the isoforms of Tai in *B. germanica* leads to precocious adult metamorphosis (Lozano et al., 2014). While Ab augments the role of Chinmo in maintaining the larval stage in *T. castaneum*, *ab* knockdown

alone does not cause precocious metamorphosis. Thus, whether Ab forms a complex with one of the Tai isoforms that interacts with Met is unclear at this point.

Ab but not Chinmo is required for larval leg regeneration

In *D. melanogaster*, Chinmo has been shown to be necessary to maintain the regenerative potential of imaginal discs (Narbonne-Reveau and Maurange, 2019). The loss of *chinmo* expression coincides with the loss of the regenerative potential of imaginal discs in late third instar larvae and induction of *br*, which promotes differentiation of imaginal discs. Misexpression of one of the *br* isoforms, *br-Z1*, leads to restricted expression of *wingless*, a marker for regeneration (Narbonne-Reveau and Maurange, 2019). Thus, in *D. melanogaster*, Chinmo promotes imaginal disc regeneration and Br appears to counteract this effect. In *T. castaneum*, we determined that *chinmo* knockdown larvae can regenerate their legs efficiently and regrow a nearly perfect pupal leg after molting into another larva (Fig. 8B). This implies that although Chinmo is necessary for inhibiting *br* expression, it does not play a major role in larval leg regeneration. Ab, in contrast, is necessary for regeneration, and this effect appears to be independent of Br since double knockdown of *ab* and *br* did not rescue the loss of regenerative potential of larval legs (Fig. 8C, D). It is possible that the distinct regenerative roles of *ab* and *chinmo* in *D. melanogaster* and *T. castaneum* may be due to differences in specific tissues and species examined: *T. castaneum* develop functional larval appendages, whereas *D. melanogaster* larvae lack appendages and instead have imaginal discs that grow internally. Moreover, Narbonne-Reveau and Maurange (2019) examined wing discs whereas in this study, we examined the effect of leg ablation. Alternatively, given that Chinmo and Ab both belong to the BTB domain transcription factor family and share similar amino acid sequences, it is possible

that the target enhancer sequences can easily evolve to selectively bind one transcription factor and not the other in a species-specific manner.

Taken together, we demonstrate that the role of *chinmo* in maintaining the larval stage is likely conserved across the Holometabola. However, tissue specific responses are evident in *T. castaneum* larvae, which have distinct life-history specific cell types. Our study also shows that Ab and Chinmo act cooperatively to regulate the transition from the larval to pupal stage. Thus, BTB domain transcription factors interact in a complex manner to regulate the transition between life history stages.

Acknowledgements

We thank Dr. Lynn Riddiford and two reviewers for their helpful comments on this manuscript. We also thank the members of the Suzuki lab for their assistance and helpful advice in completing this project, and for their helpful inputs on this manuscript. This work was supported by the National Science Foundation grant IOS-2002354 to YS and funds provided by Wellesley College.

Figure legends

Figure 1. Dorsal and lateral phenotypes of larvae injected with *amp^r*, *chinmo*, *ab*, and *chinmo* + *ab* dsRNA. (A-C’’’). *amp^r* dsRNA-injected larva after one molt. (D-F’’’) Larva injected with 1 µg *chinmo* dsRNA after one molt. (G-I’’’) Larva injected with 2 µg *chinmo* dsRNA after one molt. (J-L’’’) Larva injected with 1 µg *ab* dsRNA after one molt. (M-O’’’) Larva injected with 1 µg *chinmo* dsRNA + 1 µg *ab* dsRNA after one molt. Black arrowhead points to the ectopic wing-like structure. The first three columns are dorsal views of the whole body, the head and thorax and the second (T2) and third (T3) thoracic segments (from left to right). The last two columns are lateral views of the T2/T3 (left) and the abdomen (right). Dashed blue circles indicate the base of the bristles, which are prominent in *chinmo* + *ab* RNAi larvae. Scale bars represent 0.5 mm.

Figure 2. Ventral and lateral phenotypes of larvae injected with *amp^r*, *chinmo*, *ab*, and *chinmo* + *ab* dsRNA. (A) *amp^r* dsRNA-injected larva after one molt. (B) Larva injected with 1 µg *chinmo* dsRNA after one molt. (C) Larva injected with 2 µg *chinmo* dsRNA after one molt. (D) Larva injected with 1 µg *ab* dsRNA after one molt. (E) Larva injected with 1 µg *chinmo* dsRNA + 1 µg *ab* dsRNA after one molt. (F) Larva injected with 1 µg *chinmo* dsRNA + 1 µg *ab* dsRNA + 1 µg *br* dsRNA after one molt. Black arrowhead points to the ectopic wing-like structure. The first two columns are ventral (left) and lateral (right) views of the head and thorax. The last three columns are images of the foreleg (left), midleg (middle) and hindleg (right). Scale bars represent 0.2 mm.

Figure 3. Head morphology, feeding and ectopic wing-like projections of larvae injected with *amp^r*, *chinmo*, *ab*, and *chinmo* + *ab* dsRNA. (A) *amp^r* dsRNA-injected larva after one

molt. (B) Larva injected with 1 µg *chinmo* dsRNA after one molt. (C) Larva injected with 2 µg *chinmo* dsRNA after one molt. (D) Larva injected with 1 µg *ab* dsRNA after one molt. (E) Larva injected with 1 µg *chinmo* dsRNA + 1 µg *ab* dsRNA after one molt. (F) Gut isolated from *amp*^{r}, *chinmo*, and *chinmo* + *ab* dsRNA-injected larvae. Larvae were given flour containing red food coloring after the molt and allowed to feed for two days before the guts were isolated and imaged. (G-I'') GFP expression in *chinmo* + *ab* dsRNA injected Pu11 larva and *ab* knockdown Pu11 prepupa. GFP is absent in the wing-like projections of *chinmo* + *ab* dsRNA injected larvae (G, H) despite its presence in *ab* RNAi prepupa (I) and pupa (I''). (I') A brightfield image of the *ab* knockdown pupa shown in I'' is provided for reference. White arrowheads point to wing-like projections/wings.

Figure 4. Summary of phenotypes and molting time of larvae injected with *amp*^{r}, *chinmo*, *ab*, and *chinmo* + *ab* dsRNA. On the X-axis is the time taken for the larvae to molt after being injected with dsRNA. The Y-axis shows the range of phenotypes observed.

Figure 5. Strongly affected phenotypes of *chinmo* + *ab* double knockdown larvae. (A-A'') Pupa that developed without undergoing any additional larval-larval molts after dsRNA injection into the sixth instar larva. (B-B'') A larval-pupal intermediate that formed one molt after dsRNA injection into the sixth instar larva. (C-D'') A larval-pupal intermediate that formed one molt after dsRNA injection into the fifth instar larva. (D-D') Gin trap-like projections (black arrowhead) are seen on some of the abdominal segments (inset is a magnified view of one of these structures). (D'') A leg with pupa-like morphology. White arrowhead indicates the tip of the pupa-like leg that is still encased in the fifth instar cuticle. (E-E'') A larva with pupal traits that appeared one molt after dsRNA injection into the fifth instar larva.

552 **Figure 6. Expression of *br*, *E93* and *Kr-h1* in larvae injected with *amp*^{r}, *chinmo*, *ab*, *chinmo***
553 **+ *ab*, and *chinmo* + *ab* + *br* core dsRNA.** (A) Expression of the *br* core region. (B) Expression
554 of the *br-Z1* isoform. (C) Expression of *E93*. (D) Expression of the *Kr-h1*. Larvae were injected
555 with dsRNA on day 0 of the sixth instar and RNA was isolated 3 days later. Error bars represent
556 standard error. Each bar represents the mean of expression of three or four biological replicates.
557 Bars marked with different letters are significantly different from each other (one-way ANOVA
558 with Tukey HSD post-hoc test). Error bars are standard error bars.
559
560 **Figure 7. Methoprene does not alter the *chinmo* and *chinmo* + *ab* knockdown phenotypes**
561 **and maintains *chinmo* expression in the final instar.** (A) Acetone-treated *chinmo* RNAi larva.
562 (B) *chinmo* RNAi larva treated with 15 µg methoprene. (C) *chinmo* + *ab* RNAi larva treated with
563 15 µg methoprene. (D-E) Expression of *chinmo* (D), *Kr-h1* (E) and *ab* (F) three days after topical
564 application of acetone, 30 µg methoprene or 60 µg methoprene to day 0 final instar larvae. (G,
565 H) Knockdown of *Met*, *Kr-h1*, or *jhamt3* does not alter *chinmo* or *ab* expression. Bars marked
566 with different letters are significantly different from each other (one-way ANOVA with Tukey
567 HSD post-hoc test). Error bars are standard error bars.

568 **Figure 8. *ab* but not *chinmo* is necessary for *T. castaneum* larval leg regeneration.** (A)
569 Regenerated legs of a larva one molt after *amp*^{r} dsRNA injection. (B) Regenerated legs of a larva
570 one molt after *chinmo* dsRNA injection. (C) *ab* dsRNA-injected larva failed to regenerate its leg
571 (white arrowhead). (D) *br* RNAi does not rescue the loss of regenerative potential in the *ab*
572 dsRNA-injected larva. White arrowhead indicates the stump where a leg should have grown
573 back.

Figure 9. JH signaling is not necessary for larval leg regeneration. (A, B, C, E) *amp^r* (A), *jhamt3* (B), *Met* (C), and *Kr-h1* (E) dsRNA-injected adult with regenerated legs. (A', B', D-D'', F-F') Close-ups of the intact and regenerated legs. In all animals, dsRNA was injected into day 2 fifth instar larvae and left mid- and hindlegs were ablated on day 1 of the sixth instar. With the exception of *amp^r* dsRNA-injected adults, the ablated larvae underwent metamorphosis without undergoing any additional larval-larval molts. f = femur; ti = tibia; ta = tarsal segments.

Figure 10. Proposed summary of the major roles of Ab and Chinmo in regulating larval tissue identity and leg regeneration in *T. castaneum*. (A) The proliferation of imaginal cells, which proliferate *de novo* during metamorphosis, requires Ab / Chinmo but is inhibited by JH during the larvae stage. (B) In polymorphic cells, which contribute to both larval and adult legs, Ab and Chinmo prevent precocious expression of *br*, leading to the maintenance of larval identity. During metamorphosis, Ab / Chinmo no longer repress Br, allowing tissues to become pupally committed. Separately, regeneration of larval legs requires Ab.

589 **References**
590
591 Angelini, D.R., Kikuchi, M., Jockusch, E.L., 2009. Genetic patterning in the adult capitate
592 antenna of the beetle *Tribolium castaneum*. Dev Biol 327, 240–251.
593 Angelini, D.R., Smith, F.W., Jockusch, E.L., 2012. Extent with modification: leg patterning in
594 the beetle Tribolium castaneum and the evolution of serial homologs. G3 Bethesda 2,
595 235–48.
596 Arakane, Y., Lomakin, J., Beeman, R.W., Muthukrishnan, S., Gehrke, S.H., Kanost, M.R.,
597 Kramer, K.J., 2009. Molecular and functional analyses of amino acid decarboxylases
598 involved in cuticle tanning in Tribolium castaneum. J Biol Chem 284, 16584–16594.
599 Bryant, P.J., 1971. Regeneration and duplication following operations in situ on the imaginal
600 discs of Drosophila melanogaster. Dev Biol 26, 637–51.
601 Caygill, E.E., Johnston, L.A., 2008. Temporal regulation of metamorphic processes in
602 *Drosophila* by the *let-7* and *miR-125* heterochronic microRNAs. Curr Biol 18, 943–950.
603 Chafino S., Ureña E., Casanova J., Casacuberta E., Franch-Marro X., Martín D., 2019.
604 Upregulation of E93 gene expression acts as the trigger for metamorphosis independently
605 of the threshold size in the beetle Tribolium castaneum. Cell Rep 27, 1039-1049.e2.
606 Chafino, S., Giannios, P., Casanova, J., Martín, D., Franch-Marro, X., 2023. Antagonistic role of
607 the BTB-zinc finger transcription factors Chinmo and Broad-Complex in the
608 juvenile/pupal transition and in growth control. Elife 12.
609 Charles, J.P., Iwema, T., Epa, V.C., Takaki, K., Rynes, J., Jindra, M., 2011. Ligand-binding
610 properties of a juvenile hormone receptor, Methoprene-tolerant. Proc Natl Acad Sci U A
611 108, 21128–21133.
612 Chou, J., Ferris, A.C., Chen, T., Seok, R., Yoon, D., Suzuki, Y., 2019. Roles of Polycomb group
613 proteins Enhancer of zeste (E(z)) and Polycomb (Pc) during metamorphosis and larval
614 leg regeneration in the flour beetle Tribolium castaneum. Dev Biol 450, 34–46.
615 Clarck-Hachtel C.M., Linz D.M., Tomoyasu Y., 2013. Insights into insect wing origin provided
616 by functional analysis of vestigial in red flour beetle, Tribolium castaneum. Proc Natl
617 Acad Sci 110, 16951–16956.
618 Doggett, K., Turkel, N., Willoughby, L.F., Ellul, J., Murray, M.J., Richardson, H.E., Brumby,
619 A.M., 2015. BTB-zinc finger oncogenes are required for Ras and Notch-driven
620 tumorigenesis in Drosophila. PLoS One 10, e0132987.

621 Fox, D.T., Cohen, E., Smith-Bolton, R., 2020. Model systems for regeneration: Drosophila.
622 Development 147.
623 Gilbert, L.I., Schneiderman, H.A., 1960. The development of a bioassay for the juvenile
624 hormone of insects. Trans Am Microsc Soc 79, 38–67.
625 Hatakoshi, M., Nakayama, I., Riddiford, L.M., 1988. The induction of an imperfect
626 supernumerary larval moult by juvenile hormone analogues in Manduca sexta. J. Insect
627 Physiol. 34, 373–378.
628 Hughes, C.L., Kaufman, T.C., 2000. RNAi analysis of Deformed, proboscipedia and Sex combs
629 reduced in the milkweed bug Oncopeltus fasciatus: novel roles for Hox genes in the
630 Hemipteran head. Development 127, 3683–3694.
631 Jang, A.C.-C., Chang, Y.-C., Bai, J., Montell, D., 2009. Border-cell migration requires
632 integration of spatial and temporal signals by the BTB protein Abrupt. Nat Cell Biol 11,
633 569–579.
634 Jindra M., McKinstry W.J., Nebl T., Bittova L., Ren B., Shaw J., Phan T., Lu L., Low J.K.K.,
635 Mackay J.P., Sparrow L.G., Lovrecz G.O., Hill R.J., 2021. Purification of an insect
636 juvenile hormone receptor complex enables insights into its post-translational
637 phosphorylation. J Biol Chem 297, 101387.
638 Jindra, M., Uhlirova, M., Charles, J.P., Smykal, V., Hill, R.J., 2015. Genetic evidence for
639 function of the bHLH-PAS protein Gce/Met as a juvenile hormone receptor. PLoS Genet
640 11, e1005394.
641 Karanja, F., Sahu, S., Weintraub, S., Bhandari, R., Jaszczak, R., Sitt, J., Halme, A., 2022.
642 Ecdysone exerts biphasic control of regenerative signaling, coordinating the completion
643 of regeneration with developmental progression. Proc Natl Acad Sci U A 119.
644 Konopova, B., Jindra, M., 2008. Broad-complex acts downstream of Met in juvenile hormone
645 signaling to coordinate primitive Holometabolan metamorphosis. Development 135, 559–
646 568.
647 Konopova, B., Jindra, M., 2007. Juvenile hormone resistance gene Methoprene-tolerant controls
648 entry into metamorphosis in the beetle Tribolium castaneum. Proc Natl Acad Sci U A
649 104, 10488–10493.
650 Kramer, K.J., Morgan, T.D., Hopkins, T.L., Roseland, C.R., Aso, Y., Beeman, R.W., Lookhart,
651 G.L., 1984. Catecholamines and β-alanine in the red flour beetle, Tribolium castaneum:

652 roles in cuticle sclerotization and melanization. Insect Biochem. 14, 293–298.
653 Kucherenko, M.M., Barth, J., Fiala, A., Shcherbata, H.R., 2012. Steroid-induced microRNA let-7
654 acts as a spatio-temporal code for neuronal cell fate in the developing Drosophila brain.
655 EMBO J. 31, 4511–4523.
656 Lee, A.K., Sze, C.C., Kim, E.R., Suzuki, Y., 2013. Developmental coupling of larval and adult
657 stages in a complex life cycle: insights from limb regeneration in the flour beetle,
658 Tribolium castaneum. Evodevo 4, 20.
659 Lozano, J., Kayukawa, T., Shinoda, T., Belles, X., 2014. A role for Taiman in insect
660 metamorphosis. PLoS Genet. 10, e1004769.
661 Madeira F, Pearce M, Tivey ARN, et al. 2022. Search and sequence analysis tools services from
662 EMBL-EBI in 2022. Nucl Acids Res 50(W1), W276-W279.
663 Minakuchi C., Namiki T., Yoshiyama M., Shinoda T., 2008. RNAi-mediated knockdown of
664 *juvenile hormone acid O-methyltransferase* gene causes precocious metamorphosis in the
665 red flour beetle *Tribolium castaneum*. FEBS J 275, 2919–2931.
666 Minakuchi, C., Namiki, T., Shinoda, T., 2009. Kruppel homolog 1, an early juvenile hormone-
667 response gene downstream of Methoprene-tolerant, mediates its anti-metamorphic action
668 in the red flour beetle Tribolium castaneum. Dev Biol 325, 341–350.
669 Narbonne-Reveau, K., Maurange, C., 2019. Developmental regulation of regenerative potential
670 in Drosophila by ecdysone through a bistable loop of ZBTB transcription factors. PLoS
671 Biol. 17, e3000149.
672 Nijhout, H.F., 1998. Insect Hormones. Princeton University Press, Princeton, NJ.
673 Parthasarathy, R., Palli, S.R., 2009. Molecular analysis of juvenile hormone analog action in
674 controlling the metamorphosis of the red flour beetle, Tribolium castaneum. Arch Insect
675 Biochem Physiol 70, 57–70.
676 Parthasarathy, R., Tan, A., Bai, H., Palli, S.R., 2008a. Transcription factor broad suppresses
677 precocious development of adult structures during larval-pupal metamorphosis in the red
678 flour beetle, *Tribolium castaneum*. Mech Dev 125, 299–313.
679 Parthasarathy, R., Tan, A., Palli, S.R., 2008b. bHLH-PAS family transcription factor
680 methoprene-tolerant plays a key role in JH action in preventing the premature
681 development of adult structures during larval-pupal metamorphosis. Mech Dev 125, 601–
682 16.

683 Ravisankar, P., Lai, Y.-T., Sambrani, N., Tomoyasu, Y., 2016. Comparative developmental
684 analysis of Drosophila and Tribolium reveals conserved and diverged roles of abrupt in
685 insect wing evolution. Dev Biol 409, 518–529.
686 Riddiford, L.M., 1996. Juvenile hormone: The status of its "'status quo'" action. Arch. Insect
687 Biochem. Physiol. 32, 271–286.
688 Riddiford, L.M., Ajami, A.M., 1973. Juvenile hormone: its assay and effects on pupae of
689 Manduca sexta. J Insect Physiol 19, 749–762.
690 Riddiford, L.M., Ashburner, M., 1991. Effects of juvenile hormone mimics on larval
691 development and metamorphosis of Drosophila melanogaster. Gen Comp Endocrinol 82,
692 172–183.
693 Schubiger, G., 1971. Regeneration, duplication and transdetermination in fragments of the leg
694 disc of Drosophila melanogaster. Dev Biol 26, 277–95.
695 Suzuki, Y., Chou, J., Garvey, S.L., Wang, V.R., Yanes, K.O., 2019. Evolution and Regulation of
696 Limb Regeneration in Arthropods, in: Tworzydlo, W., Bilinski, S.M. (Eds.), Evo-Devo:
697 Non-Model Species in Cell and Developmental Biology. Springer International
698 Publishing, Cham, pp. 419–454.
699 Suzuki, Y., Squires, D.C., Riddiford, L.M., 2009. Larval leg integrity is maintained by Distal-
700 less and is required for proper timing of metamorphosis in the flour beetle, Tribolium
701 castaneum. Dev Biol 326, 60-7.
702 Suzuki, Y., Truman, J.W., Riddiford, L.M., 2008. The role of broad in the development of
703 *Tribolium castaneum*: implications for the evolution of the holometabolous insect pupa.
704 Development 135, 569–577.
705 Tan, A., Palli, S.R., 2008. Edysone receptor isoforms play distinct roles in controlling molting
706 and metamorphosis in the red flour beetle, Tribolium castaneum. Mol Cell Endocrinol
707 291, 42–49.
708 Truman, J.W., 2019. The Evolution of Insect Metamorphosis. Curr Biol 29, R1252–R1268.
709 Truman, J.W., Riddiford, L.M., 2022. Chinmo is the larval member of the molecular trinity that
710 directs Drosophila metamorphosis. Proc Natl Acad Sci U A 119, e2201071119.
711 Turkel, N., Sahota, V.K., Bolden, J.E., Goulding, K.R., Doggett, K., Willoughby, L.F., Blanco,
712 E., Martin-Blanco, E., Corominas, M., Ellul, J., Aigaki, T., Richardson, H.E., Brumby,
713 A.M., 2013. The BTB-zinc finger transcription factor abrupt acts as an epithelial

oncogene in Drosophila melanogaster through maintaining a progenitor-like cell state. PLoS Genet 9, e1003627.

Urena, E., Manjon, C., Franch-Marro, X., Martin, D., 2014. Transcription factor E93 specifies adult metamorphosis in hemimetabolous and holometabolous insects. Proc Natl Acad Sci U A 111, 7024–9.

Villarreal, C.M., Darakananda, K., Wang, V.R., Jayaprakash, P.M., Suzuki, Y., 2015. Hedgehog signaling regulates imaginal cell differentiation in a basally branching holomextabolous insect. Dev Biol 404, 125–135.

Wu, Y.-C., Chen, C.-H., Mercer, A., Sokol, N.S., 2012. Let-7-complex microRNAs regulate the temporal identity of Drosophila mushroom body neurons via chinmo. Dev Cell 23, 202–209.

Zhou, B., Hiruma, K., Shinoda, T., Riddiford, L.M., 1998. Juvenile hormone prevents ecdysteroid-induced expression of *broad complex* RNAs in the epidermis of the tobacco hornworm, *Manduca sexta*. Dev Biol 203, 233–244.

Zhou, B., Riddiford, L.M., 2001. Hormonal regulation and patterning of the Broad-Complex in the epidermis and wing discs of the tobacco hornworm, Manduca sexta. Dev Biol 231, 125–137.

Zhou, X., Riddiford, L.M., 2002. Broad specifies pupal development and mediates the "*status quo*" action of juvenile hormone on the pupal-adult transformation in *Drosophila* and *Manduca*. Development 129, 2259–2269.

Zhu, S., Lin, S., Kao, C.F., Awasaki, T., Chiang, A.S., Lee, T., 2006. Gradients of the Drosophila Chinmo BTB-zinc finger protein govern neuronal temporal identity. Cell 127, 409–22.

Figure 1

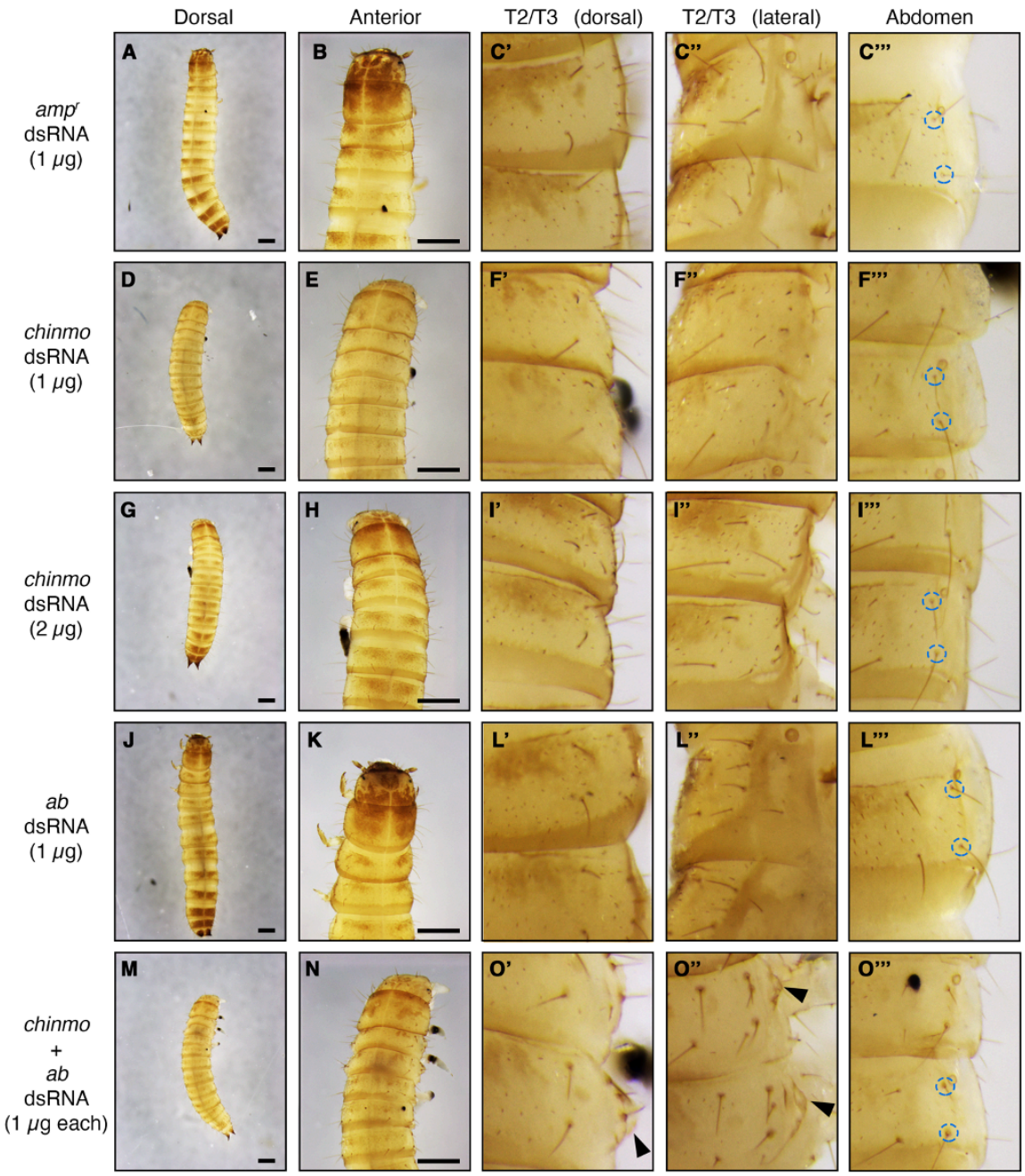

739

740

Figure 2

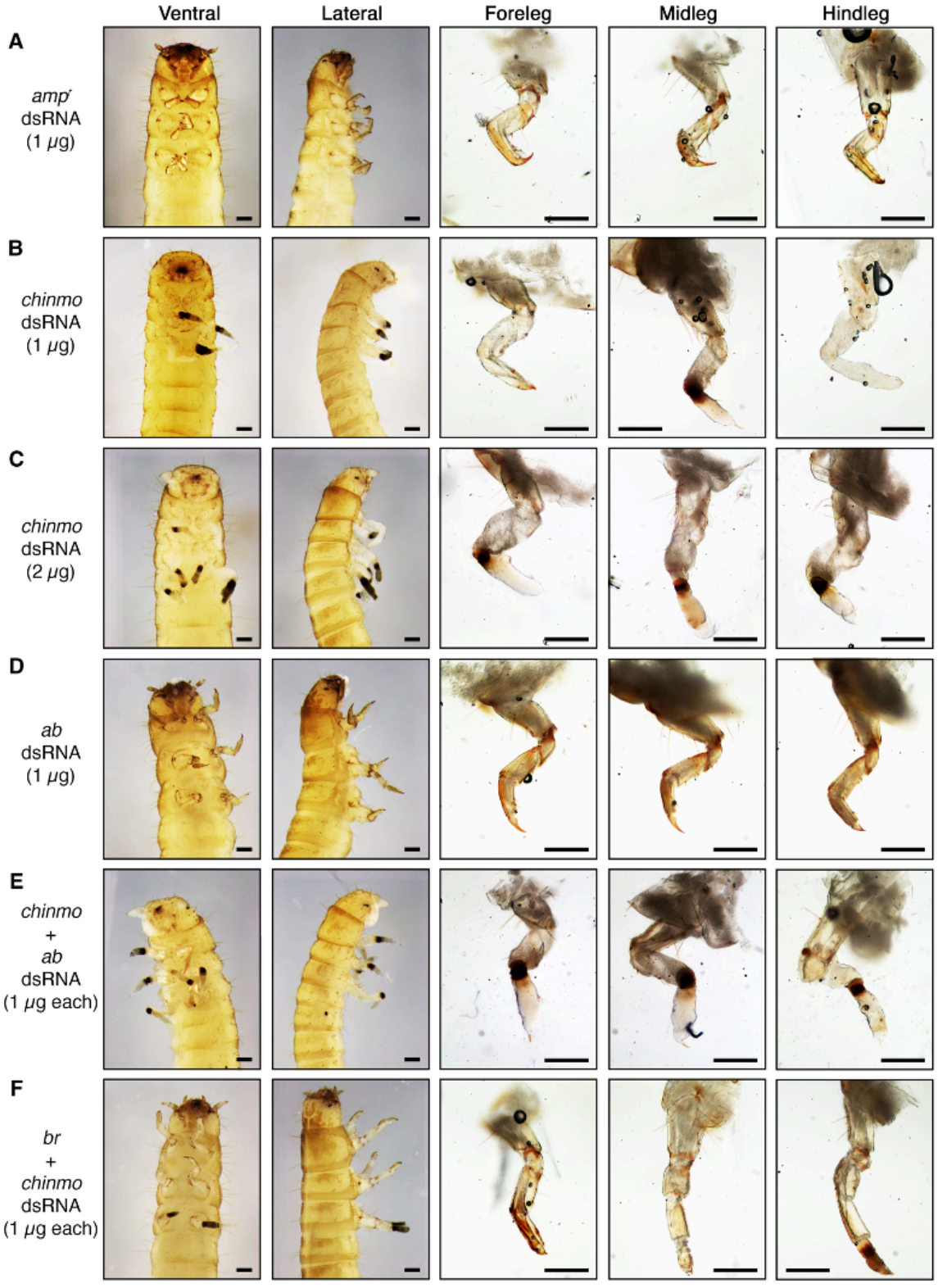
Ventral
Lateral
Foreleg
Midleg
Hindleg
A
amp dsRNA (1 μg)
B
chinmo dsRNA (1 μg)
C
chinmo dsRNA (2 μg)
D
ab dsRNA (1 μg)
E
chinmo + ab dsRNA (1 μg each)
F
br + chinmo dsRNA (1 μg each)

741

Figure 3

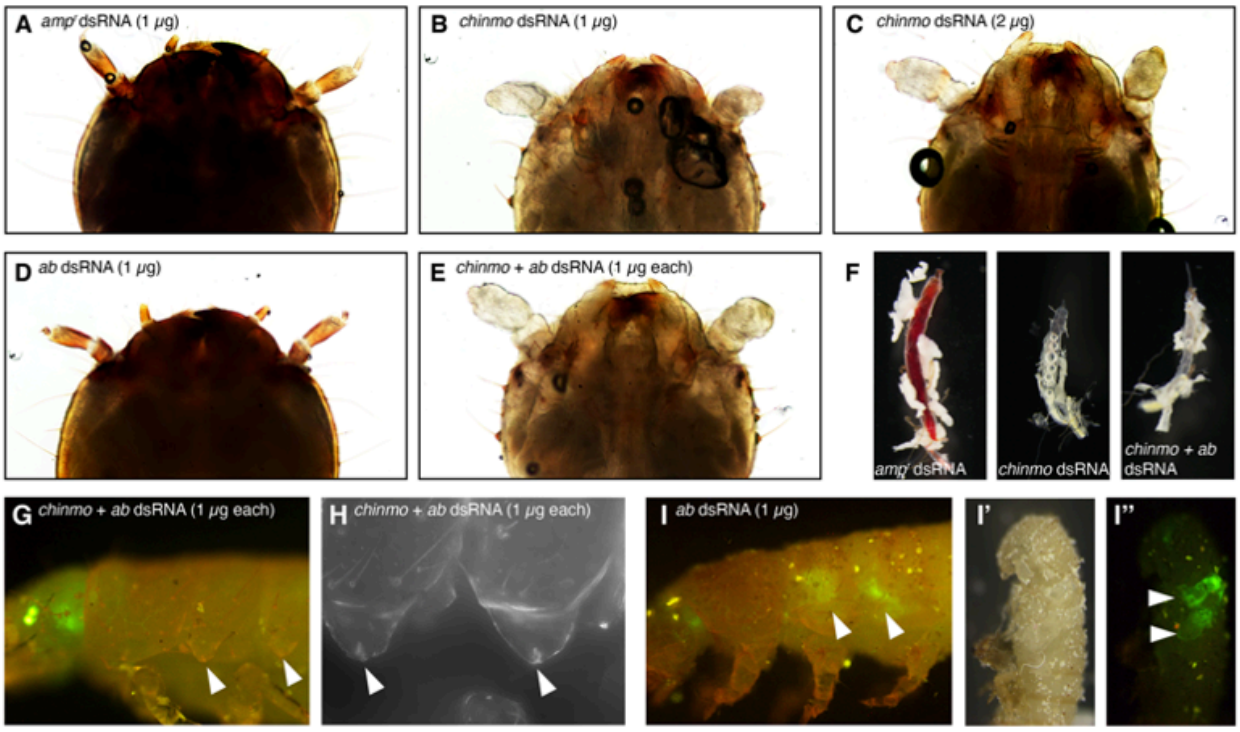
A amp' dsRNA (1 µg)
B chinmo dsRNA (1 µg)
C chinmo dsRNA (2 µg)
D ab dsRNA (1 µg)
E chinmo + ab dsRNA (1 µg each)
F
amp' dsRNA
chinmo dsRNA
chinmo + ab dsRNA
G chinmo + ab dsRNA (1 µg each)
H chinmo + ab dsRNA (1 µg each)
I ab dsRNA (1 µg)
I'
I''

742

Figure 4

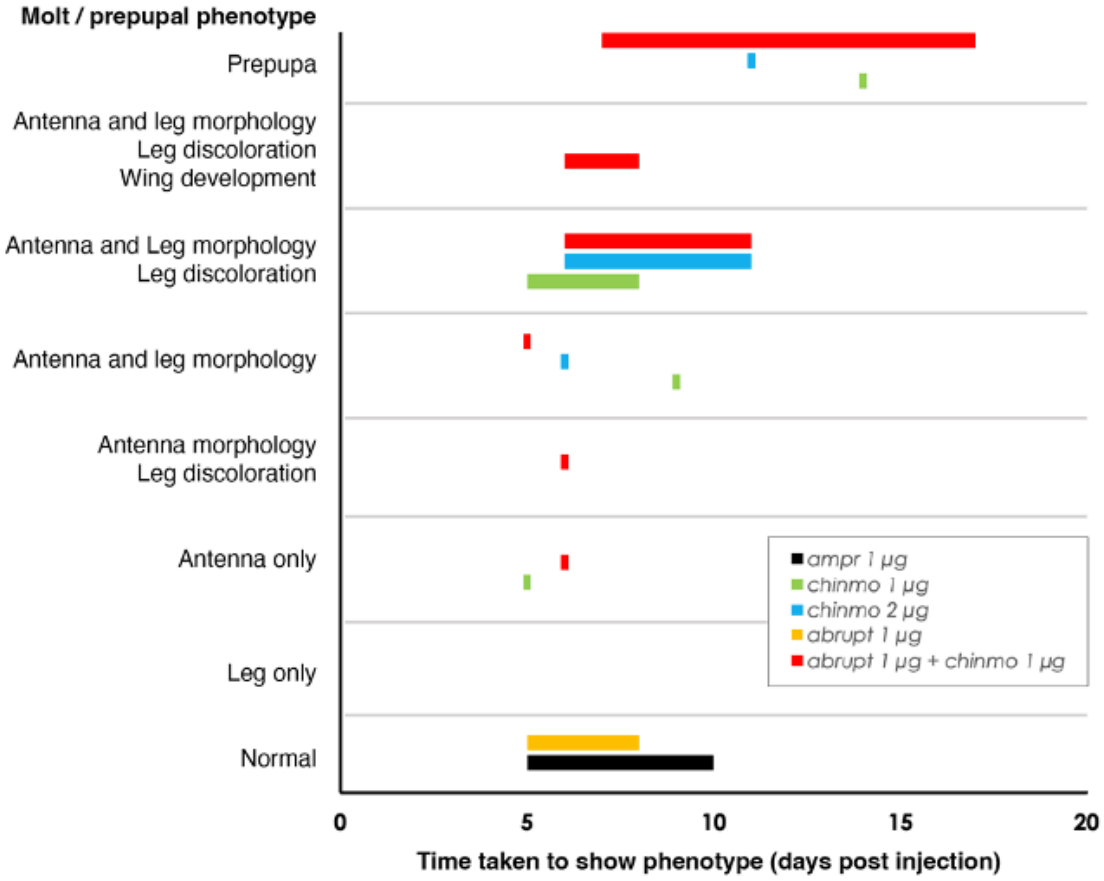
Molt / prepupal phenotype
Prepupa
Antenna and leg morphology
Leg discoloration
Wing development
Antenna and Leg morphology
Leg discoloration
Antenna and leg morphology
Antenna morphology
Leg discoloration
Antenna only
Leg only
Normal
ampr 1 µg
chinmo 1 µg
chinmo 2 µg
abrupt 1 µg
abrupt 1 µg + chinmo 1 µg
0
5
10
15
20
Time taken to show phenotype (days post injection)

743

Figure 5

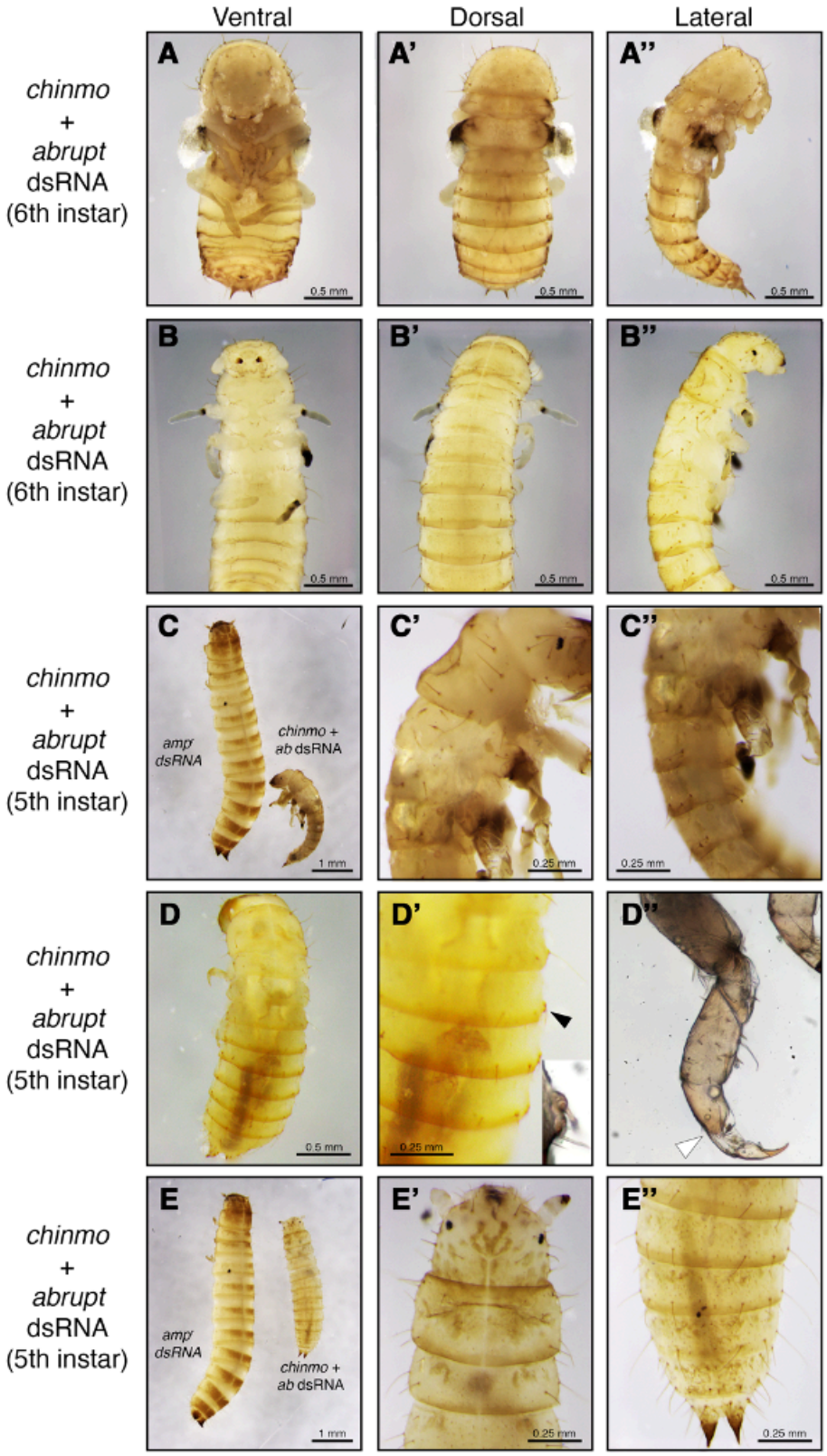
Ventral
Dorsal
Lateral
chinmo + abrupt dsRNA (6th instar)
chinmo + abrupt dsRNA (6th instar)
chinmo + abrupt dsRNA (5th instar)
chinmo + abrupt dsRNA (5th instar)
chinmo + abrupt dsRNA (5th instar)
A
A'
A''
B
B'
B''
C
C'
C''
D
D'
D''
E
E'
E''
amp dsRNA
chinmo + ab dsRNA
amp dsRNA
chinmo + ab dsRNA
0.5 mm
1 mm
0.25 mm

744

Figure 6

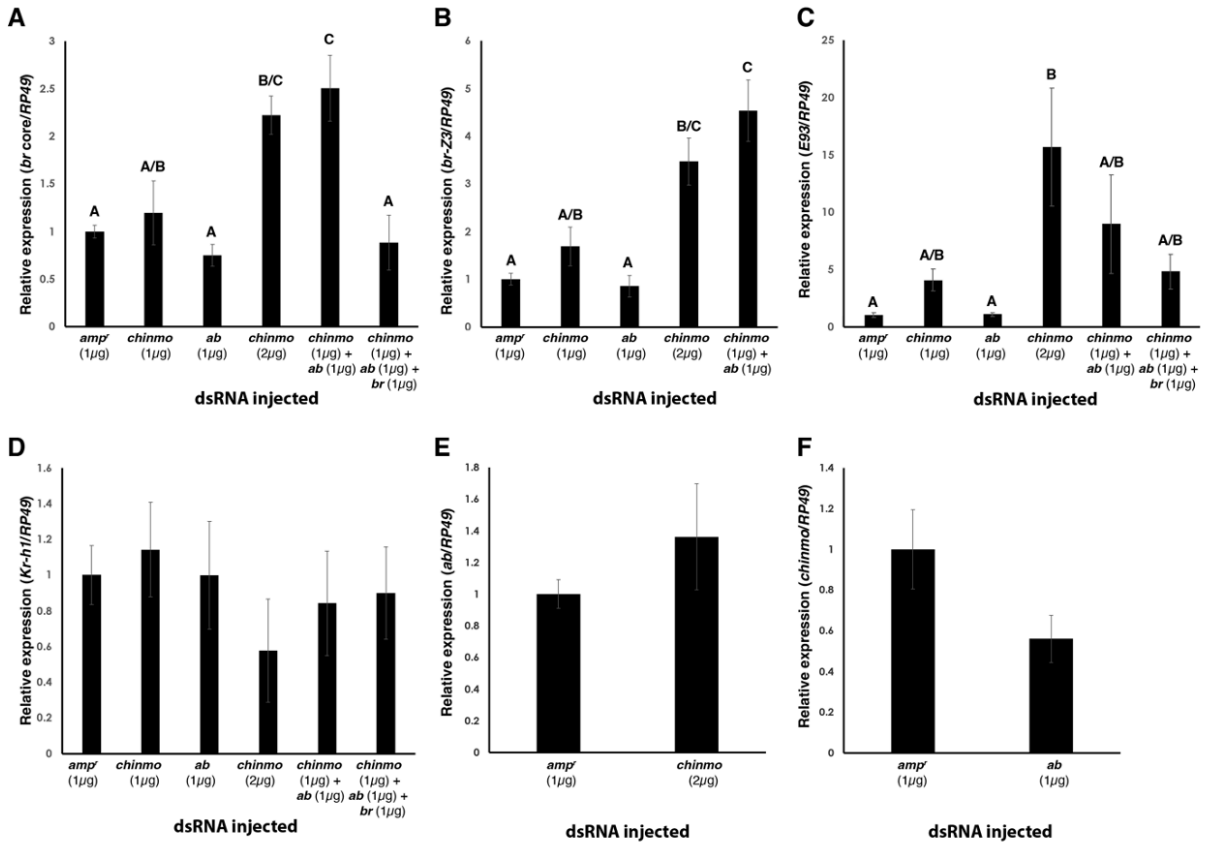
A
Relative expression (br core/RP49)
A
A/B
A
B/C
C
A
amp' (1μg)
chinmo (1μg)
ab (1μg)
chinmo (2μg)
chinmo (1μg) + ab (1μg)
chinmo (1μg) + ab (1μg) + br (1μg)
dsRNA injected
B
Relative expression (br-Z3/RP49)
A
A/B
A
B/C
C
amp' (1μg)
chinmo (1μg)
ab (1μg)
chinmo (2μg)
chinmo (1μg) + ab (1μg)
dsRNA injected
C
Relative expression (E93/RP49)
A
A/B
A
B
A/B
A/B
amp' (1μg)
chinmo (1μg)
ab (1μg)
chinmo (2μg)
chinmo (1μg) + ab (1μg)
chinmo (1μg) + ab (1μg) + br (1μg)
dsRNA injected
D
Relative expression (Kr-h1/RP49)
amp' (1μg)
chinmo (1μg)
ab (1μg)
chinmo (2μg)
chinmo (1μg) + ab (1μg)
chinmo (1μg) + ab (1μg) + br (1μg)
dsRNA injected
E
Relative expression (ab/RP49)
amp' (1μg)
chinmo (2μg)
dsRNA injected
F
Relative expression (chinmo/RP49)
amp' (1μg)
ab (1μg)
dsRNA injected

745

Figure 7

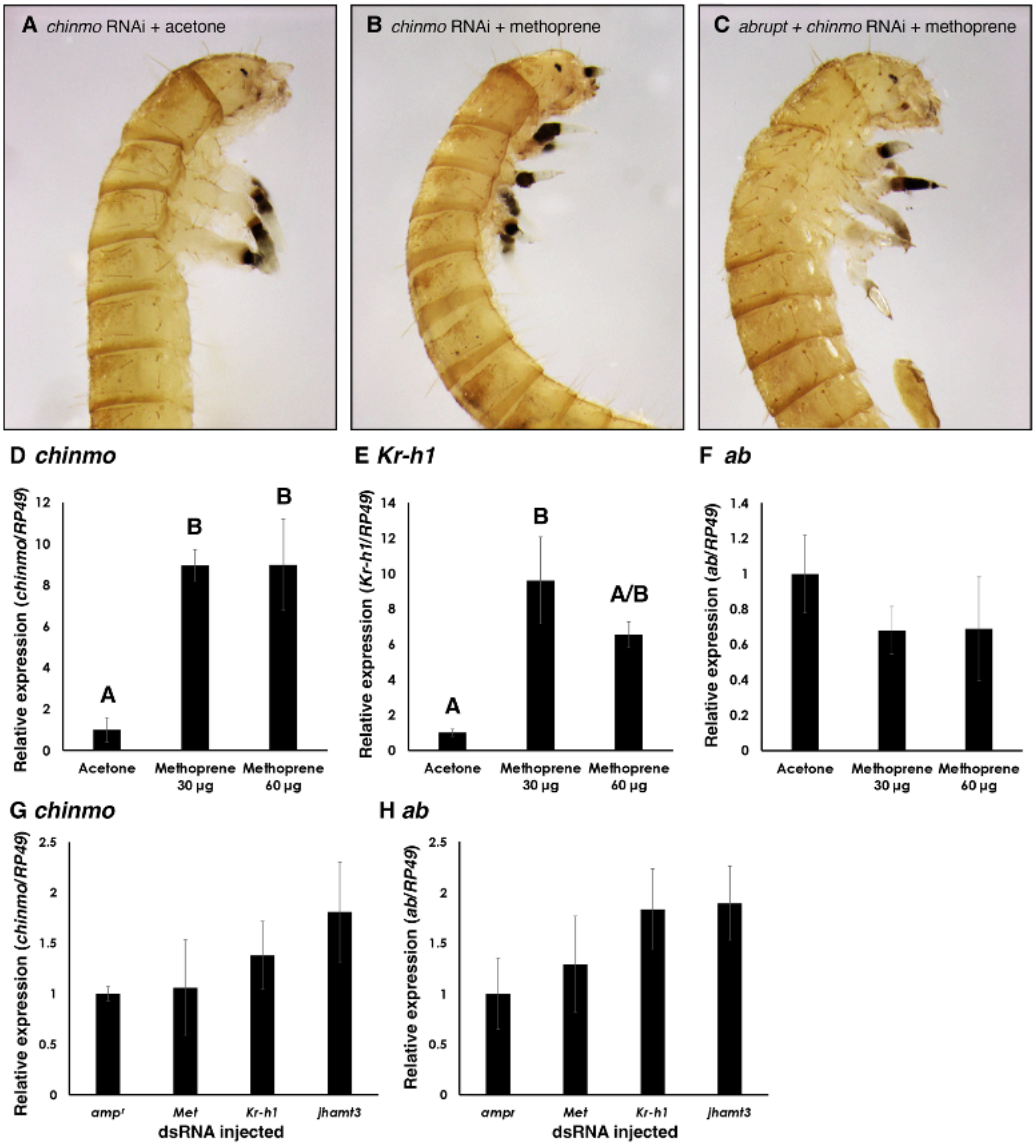
A chinmo RNAi + acetone
B chinmo RNAi + methoprene
C abrupt + chinmo RNAi + methoprene
D chinmo
E Kr-h1
F ab
Relative expression (chinmo/RP49)
Relative expression (Kr-h1/RP49)
Relative expression (ab/RP49)
A
B
B
A
B
A/B
Acetone
Methoprene 30 µg
Methoprene 60 µg
G chinmo
H ab
ampr
Met
Kr-h1
Jhamt3
dsRNA injected

746

Figure 8

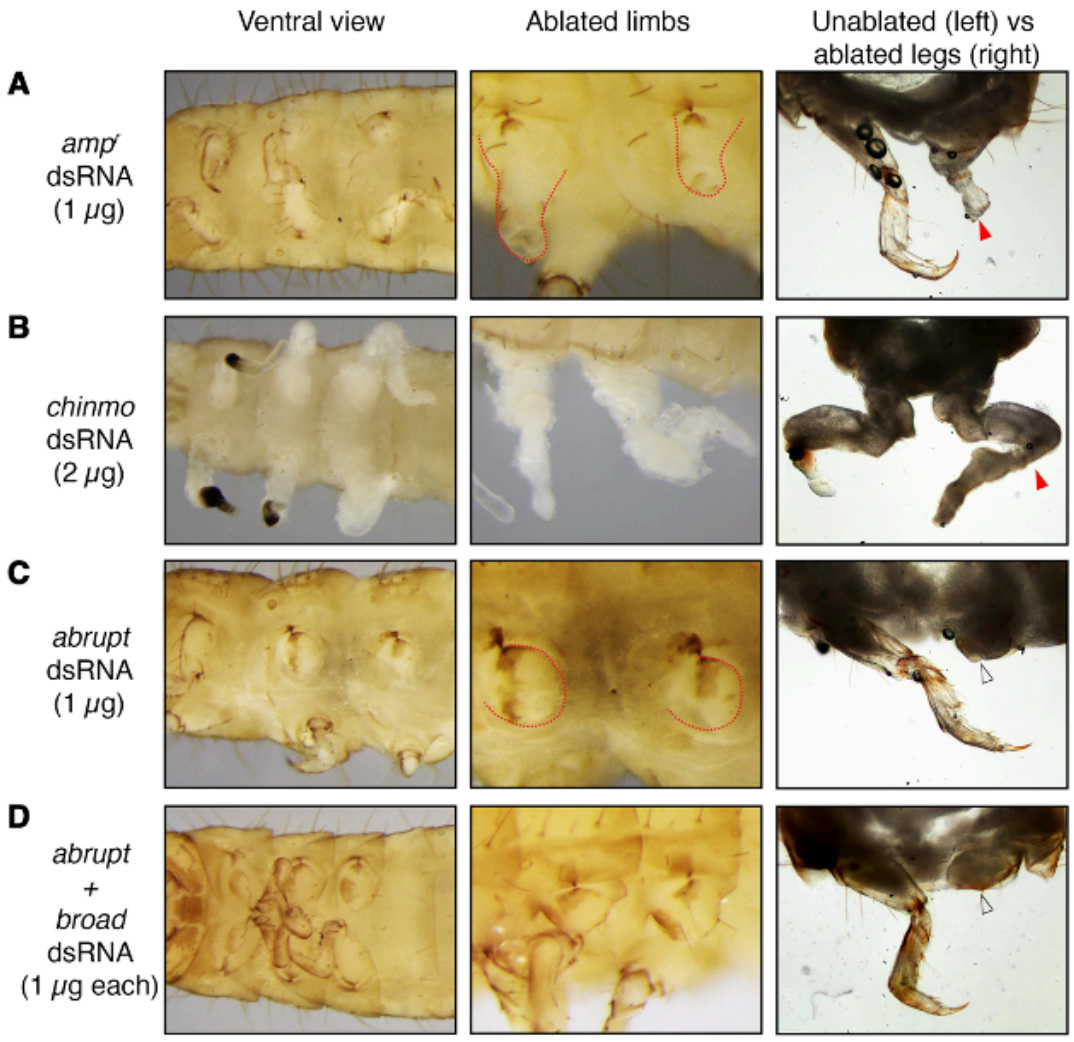
Ventral view
Ablated limbs
Unablated (left) vs ablated legs (right)
A
amp' dsRNA (1 μg)
B
chinmo dsRNA (2 μg)
C
abrupt dsRNA (1 μg)
D
abrupt + broad dsRNA (1 μg each)

747

Figure 9

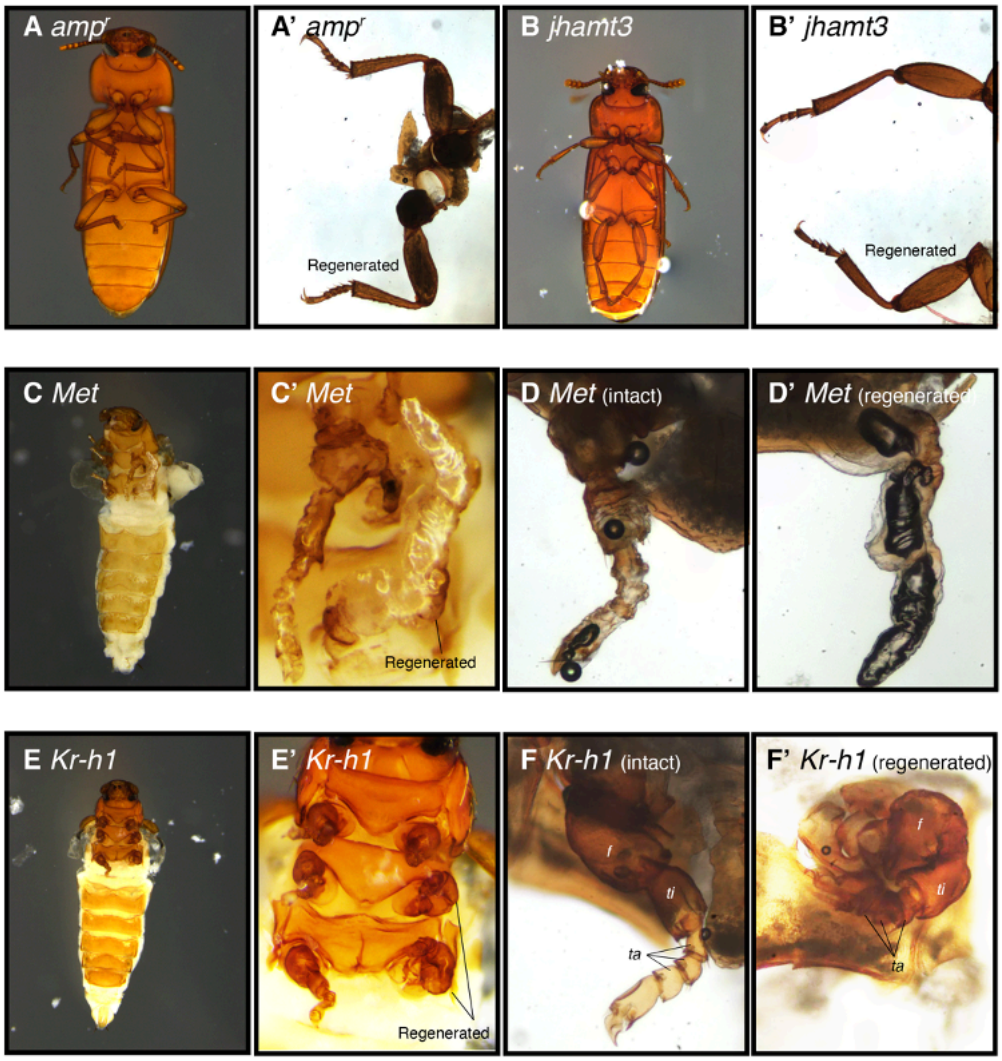
A amp^r
A' amp^r
Regenerated
B jhamt3
B' jhamt3
Regenerated
C Met
C' Met
Regenerated
D Met (intact)
D' Met (regenerated)
E Kr-h1
E' Kr-h1
Regenerated
F Kr-h1 (intact)
f
ti
ta
F' Kr-h1 (regenerated)
f
ti
ta

748

Figure 10

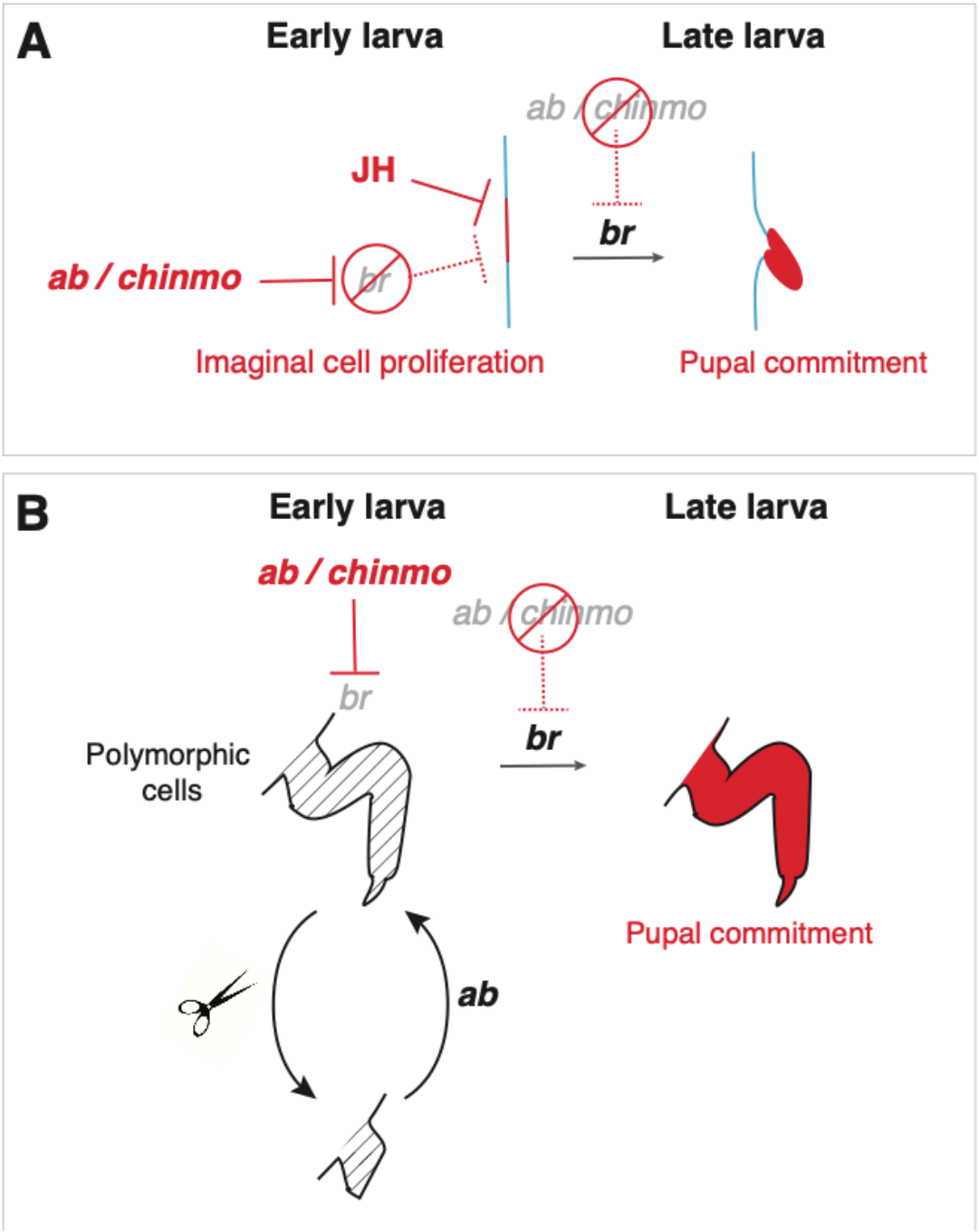

749